Supplemental Methods

Essential Role of HIPK2 in TGFβ–dependent survival of midbrain dopamine neurons.

Jiasheng Zhang, Vanee Pho, Stephen J Bonasera, Jed Holzmann, Joanna Hellmuth, Amy T Tang, Siuwah Tang, Patricia H Janak, Laurence H Tecott & Eric J Huang

Gene targeting of *Hipk2* and generation of *Hipk2*$^{-/-}$ mutant mice. *Hipk2*$^{-/-}$ null mice have been previously described[1]. *Tgfβ1*$^{-/-}$ and *Tgfβ3*$^{-/-}$ mice were obtained from Dr. R. Akhurst and Dr. T. Doetschman, respectively. Animal care was approved by the Institutional of Animal Care and Use Committee and followed the National Institute of Health guidelines. For quantification of dopamine, striatum was dissected fresh from P28 mice and immediately kept frozen in dry ice. After dissection, catecholamines were acid extracted and dopamine was measured using reverse phase HPLC.

Histology and Immunohistochemistry. Mouse embryos, from E11.5 to E17.5, were fixed with 4% PFA in PBS (1% PFA for anti–activated caspase 3 antibody). Mice at postnatal day P0, P14, P28 and 10–month old were transcardially perfused with 4% PFA. Brains from these mice were fixed in 4% PFA overnight at 4°C, cryoprotected in 15%–30% sucrose overnight and sectioned in the coronal plane using a cryostat. Brains from embryos and P0 mice were section at 20 μm thickness, and those from P14, P28 and 10–month old mice were cut at 40 μm, free–floated in PBS and mounted on Superfrost glass slides. Sections were stained for rabbit anti–Brn3a (1:1,000)[1, 2] or anti–TH antibody (1:500; Chemicon) in blocking solution overnight at room

temperature, rinsed in TBS, and then incubated for 1 h with biotinylated anti–rabbit IgG (1:300; Vector Laboratories). After three washes, sections were incubated for 1 hr at room temperature in blocking solution containing avidin–biotin complex. Visualization of the product was performed using DAB (Sigma). Adjacent sections were stained with Cresyl Violet to reveal anatomical landmarks in the brains. Sections from the SNpc of E17.5 and P28 were incubated in LacZ staining solution for 2 h at 37°C. Expression of different TGFβ isoforms was determined using antibodies specific for TGFβ1 and TGFβ3 (R&D Systems).

To determine the number of neurons undergoing apoptosis during E14.5, E17.5 and P0, sections were double labeled with anti-TH (mAb, 1:200, Calbiochem) and anti-activated caspase 3 antibodies (rabbit polyclonal, 1:1,000, R&D Systems), followed by simultaneous incubation with secondary antibodies, Alexa 488–conjugated goat anti–mouse IgG and Alexa 568 goat anti–rabbit IgG (1:300; Molecular Probes). For neuronal birth-dating experiments, sections were incubated with rabbit anti–TH antibody and mouse anti–BrdU antibody (1:1,000, Nova Castra). To examine the co-expression of HIPK2^{lacZ} and TH, sections were incubated with anti-TH antibody and anti-β-galactosidase antibody (mAb, 1:1,000, Promega), followed by simultaneous incubation with secondary antibodies, Alexa 488–conjugated goat anti–rabbit IgG and Alexa 568 goat anti–mouse IgG. Tissue sections were examined using the BX41 Olympus microscope (Olympus) equipped with a CCD camera, Olympus DP70. Images were captured using Olympus DP Controller software program and imported into Photoshop 7.0.1 (Adobe). Confocal images were captured using the Leica confocal microscope (TCS SP, Leica). Laser intensity (measured as the PMT levels) for each fluorophor was kept within the linear range.

Locomotor Activity Tests. For the four–limb akinesia test, mice were placed on a brightly lit table and the amount of time taken for the animals to move all four limbs was monitored. Negative geotaxis was measured by placing the mice head–down on a tilted 60° cardboard platform. The time taken for the mouse to move toward the top of the platform was measured. For the tail suspension test, mice were suspended by their tails for 2 min. The presence of and the duration of hindlimb clasping were recorded. Hindlimb stride length was measured by a method adapted by Ferragut et al[3]. Hind paws of *wild type* and *Hipk2*$^{-/-}$ mutant mice were wetted with India ink. Animals were then placed on a strip of 3MM filter paper (4.5 cm wide, 40 cm long). Stride lengths were measured as the distance between two hind paw prints. Mice were placed on a 6 cm diameter rod (Model 720A, IITC/Life Science Instruments**)** accelerated from 0 to 40 revolutions per minute over 5 minutes. Mice received three 5 min trials with a 2 h inter–trial interval for 8 days. The amount of time spent on the rod before falling off was measured.

Luciferase assays. Luciferase assays were performed in 293HEK cells according to previously published protocols[4]. Deletion and point mutations of HIPK2 were generated using QuikChange Mutagenesis Kit (Stratagene) and subcloned into pRK expression vectors. For each assay, 5 ng of *Renilla* luciferase plasmids pGL4.74[hRluc–TK] (Promega) were co–transfected to serve as internal controls. Relative luciferase activities were measured using the Dual–Luciferase Assay System (Promega) and presented by normalizing firefly luciferase activities with *Renilla* luciferase activities.

References:

1. Wiggins, A. K. et al. Interaction of Brn3a and HIPK2 mediates transcriptional repression of sensory neuron survival. J Cell Biol 167, 257-67 (2004).

2. Huang, E. J. et al. POU domain factor Brn-3a controls the differentiation and survival of trigeminal neurons by regulating Trk receptor expression. Development 126, 2869-82 (1999).
3. Fernagut, P. O., Diguet, E., Labattu, B. & Tison, F. A simple method to measure stride length as an index of nigrostriatal dysfunction in mice. J Neurosci Methods 113, 123-30 (2002).
4. Lin, A. H. et al. Global analysis of Smad2/3-dependent TGF-beta signaling in living mice reveals prominent tissue-specific responses to injury. J Immunol 175, 547-54 (2005).

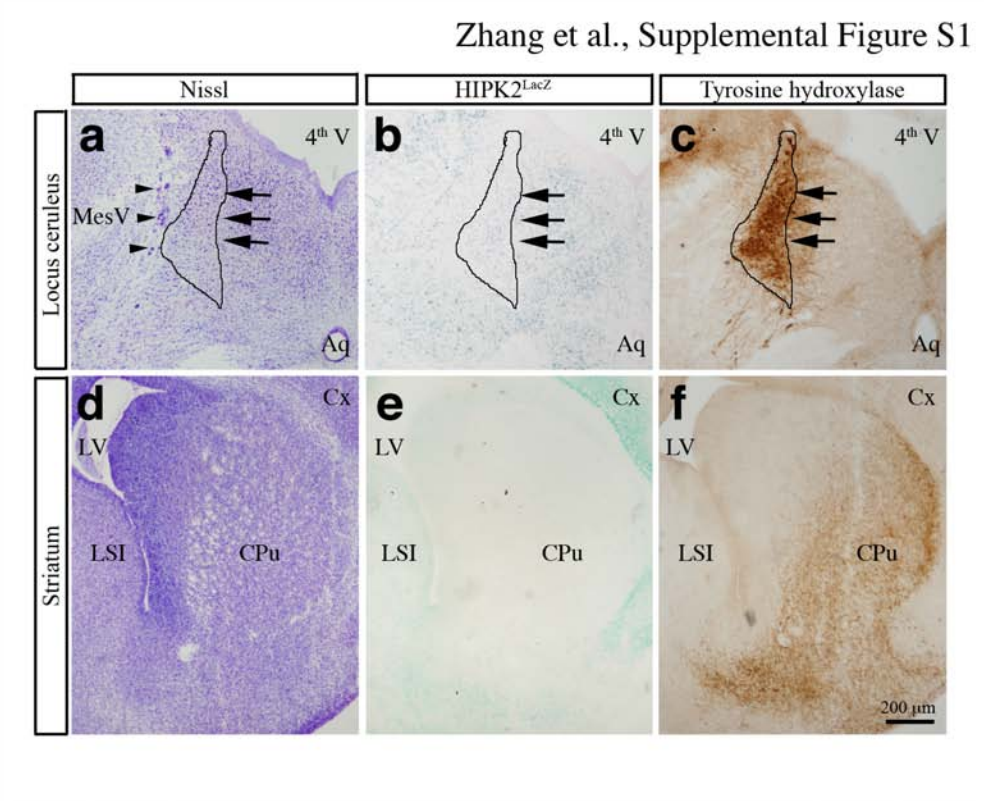

Figure S1. Absence of HIPK2 expression in locus ceruleus and striatum. (a–c) Expression of HIPK2 in locus ceruleus, a nucleus enriched with TH^+, catecholaminerigic neurons, was determined using LacZ staining, which showed essentially no detectable presence of LacZ activity. Panels a and c showed the location of locus ceruleus using Nissl stain and tyrosine hydroxylase immunohistochemistry, respectively. The region for locus ceruleus was highlighted by arrows and the mesencephalic trigeminal nucleus (MesV) by arrowheads. (d–f) Similar to the locus ceruleus, $HIPK2^{LacZ}$ was not detected in the caudate/putamen (CPu) region of the striatum, but can be detected in the cerebral neocortex (Cx). Abbreviations: 4th V: fourth ventricle, Aq: cerebral aqueduct, MesV: mesencephalic trigeminal nucleus, Cx: cerebral neocortex, LV, lateral ventricle, CPu: caudate/putamen, LSI: lateral septal nucleus, intermediate part. Scale bar, 200 μm.

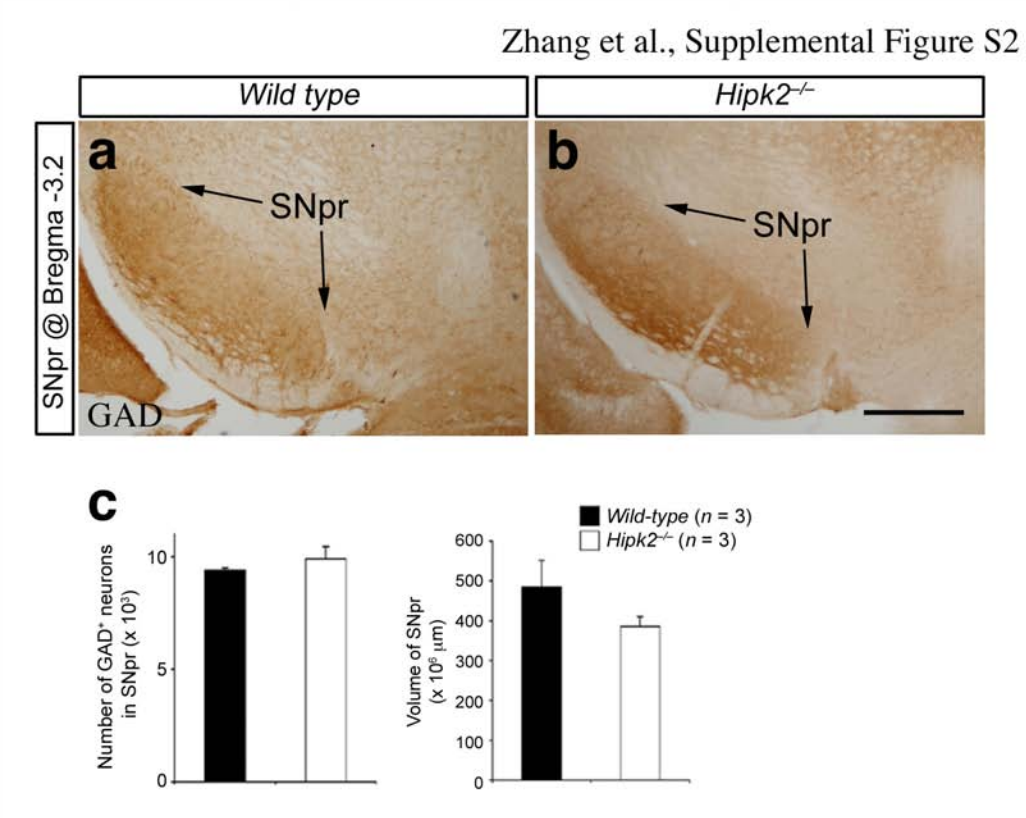

Figure S2. No detectable reduction in the number of GABAergic neurons (panel a) or the entire volume (panel b) of substantia nigra pars reticularis (SNpr). The number of GAD^+ neurons and the volume of SNpr were determined using the StereoInvestigator software (MicroBrightField). Student's *t* test, $n = 3$ for *wild-type* and $Hipk2^{-/-}$ mutants.

Zhang et al., Supplemental Figure S3

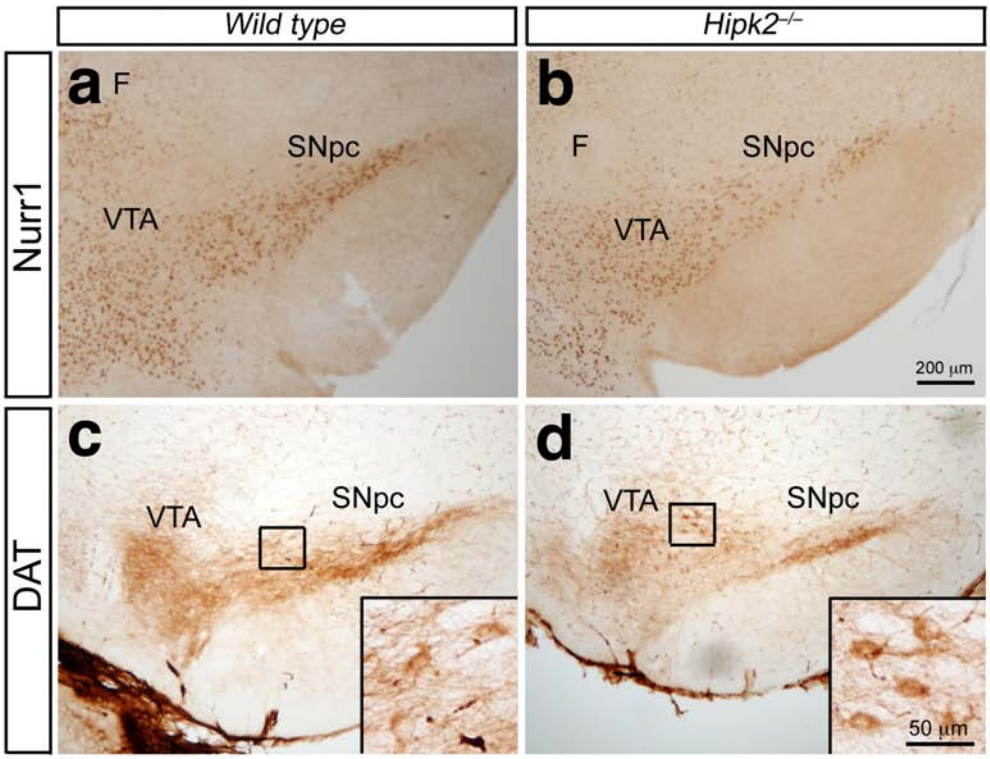

Figure S3. Loss of HIPK2 has no negative impact on the expression of cell fate or differentiation markers for DA neurons. (a,b) Expression of cell fate markers Nurr1 in the DA neurons in *wild-type* and *Hipk2*$^{-/-}$ mutants at P28 shows no detectable difference (n = 3). (c,d) Similarly, expression of DA transporter (DAT) also shows no difference in SNpc and VTA of *wild-type* and *Hipk2*$^{-/-}$ mutants at P14. Scale bar for panels a–d, 200 μm and for inset in panels c–d, 50 μm.

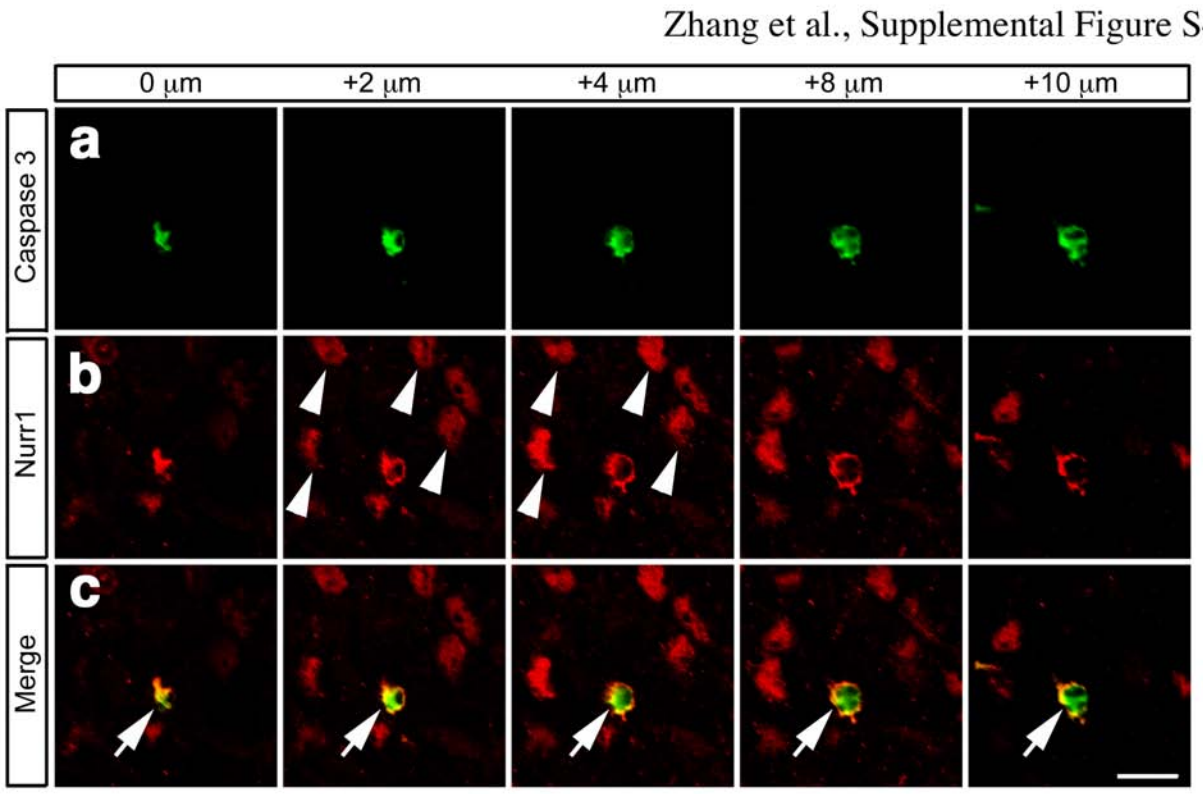

Figure S4. Co-localization of DA neuron marker Nurr1 and activated caspase 3 in SNpc of P0 *Hipk2*$^{-/-}$ mutants. (a–c) Confocal microscopic analyses are performed using double immunofluorescence for Nurr1 and caspase 3. Many of the surviving (arrowheads) and apoptotic neurons (arrow) continue to express DA neuron marker Nurr1. Scale bars in panel c, 25 μm.

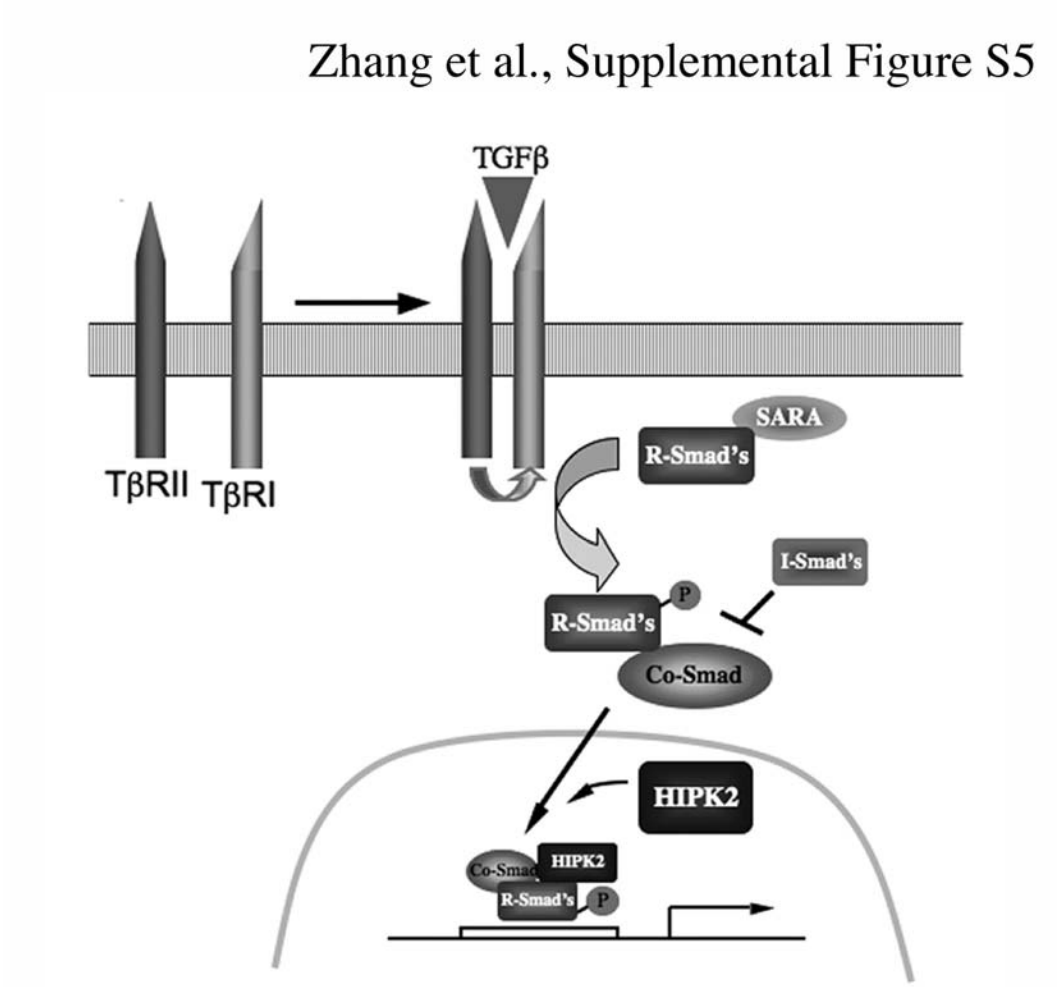

Figure S5. A working model for HIPK2 in the downstream signaling pathway of TGFβ. In this model, we propose that HIPK2 directly interacts with R-Smads and activates downstream targets of R-Smads.

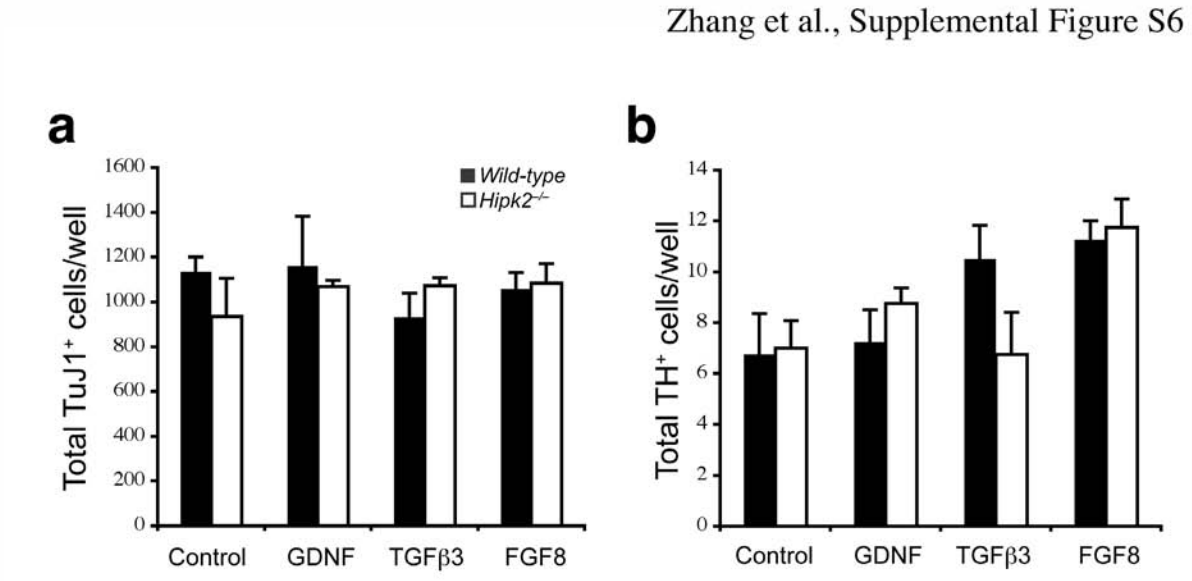

Figure S6. Determination of total TuJ1–positive and TH–positive neuron numbers in ventral mesencephalon cultures. Cultures are collected 2 hours after plating, fixed in ice-cold methanol for 15 minutes, and stained with either anti-TuJ1 or anti-TH antibodies. The total numbers of TuJ1-positive cells (panel a) and TH-positive cells (panel b) in the entire cover slides are determined under a Nikon fluorescent microscope. Numbers are presented as mean ± SEM from three embryos for *wild-type* and *Hipk2*$^{-/-}$ mutants.

Supplemental Table 1

While both *Hipk2* and *Tgfβ3* mutants are maintained in C57B6;129SvJ background, *Tgfβ1* homozygous (*Tgfβ1*$^{-/-}$) mutants in this background suffer from severe wasting syndrome and die within 3 weeks after birth[1]. When crossed into the inbred NIH-Olac background, *Tgfβ1*$^{-/-}$ mutants survive more than 2 months, making it possible to study the roles of TGFβ1 in tumorigenesis and CNS functions[2, 3].

Despite the differences in genetic background, the number of DA neurons in SNpc and VTA of wild type mice for each mutant show no significant differences (as outlined below). Importantly, all the comparisons are made using *wild-type* and mutants within each knockout line and therefore should have the same genetic background. By doing so, we minimize any negative impact on data analyses.

	Background	P0 SNpc	P0 VTA	P28 SNpc	P28 VTA
HIPK2 WT (n=3)	C57B6;129SvJ	1361 ± 127	1898 ± 370	3695 ± 224	3463 ± 476
TGFβ1 WT (n=3)	NIH/Olac	ND*	ND*	3069 ± 445	2630 ± 379
TGFβ3** WT (n=4)	C57B6;129SvJ	1138 ± 137	1975 ± 134	ND*	ND*
ANOVA		$P = 0.245$	$P = 0.831$	$P = 0.277$	$P = 0.243$

*ND, not done. **TGFβ3 homozygous mutants are perinatal lethal due to branchial arch defects.

References:

1. Shull, M. M. et al. Targeted disruption of the mouse transforming growth factor-beta 1 gene results in multifocal inflammatory disease. Nature 359, 693-9 (1992).
2. Cui, W. et al. TGFbeta1 inhibits the formation of benign skin tumors, but enhances progression to invasive spindle carcinomas in transgenic mice. Cell 86, 531-42 (1996).
3. Brionne, T. C., Tesseur, I., Masliah, E. & Wyss-Coray, T. Loss of TGF-beta 1 leads to increased neuronal cell death and microgliosis in mouse brain. Neuron 40, 1133-45 (2003).